INTERNATIONAL CAVITATION EROSION TEST SEMINAR
Sopot, 1-2nd June 2000

INVESTIGATION OF CAVITATION EROSION OF THE PA2 ALUMINIUM ALLOY

Alicja Krella

Institute of Fluid-Flow Machinery of the Polish Academy of Sciences,
Gdańsk, Poland

Abstract: *The effects of some mechanical factors on the distribution of cavitation pulses, their maximum pressure, material impingement, and erosion curves (mass decrease in time) of the PA2 aluminium alloy specimens are reviewed. The increase of the energy flux index delivered to the material by a factor of two and half results in an increase of weight loss in the PA2 alloy by a factor of over 5 after 30 hours of exposure in a cavitation tunnel with an Erdmann-Jesnitzer test chamber. Close correlation between the number of pits, their size and the increase of the energy flux delivered to the material is shown.*

1. INTRODUCTION

Cavitation erosion is known to be caused by mechanical action of pressure pulses resulting from the collapse of cavities filled with vapour or gas/vapour mixture. The amplitude of these pulses is sufficient to cause local plastic deformation of a solid material. Additionally, the cumulative liquid jet blowing at the solid surface with velocity of over 100 m/s [1] behaves like a solid, which facilitates the damage. Typically, the following phenomena can be distinguished in the cavitation erosion process. At first, slip bands appear which develop into pits. Next, the slips increase and micro-cracks are initiated. This causes surface roughness increase and also accelerates crack propagation .

One of materials tested under the International Cavitation Erosion Test (ICET) Programme, was the PA2 aluminium alloy. PA2 is a plastic material with the following mechanical properties: yield stress 169 MPa, tensile strength 208 MPa, hardness HV_{10} 71.1. Due to its low cavitation erosion strength, the PA2 alloy was tested at almost all facilities included in the ICET project.

The objective of this paper is to compare the weight loss of PA2 aluminium alloy in erosion test to the density of the energy flux delivered to the material by imploding cavities. Because of very small dimensions of implosion zones (10^{-5} m [1]) and fast rise of pressure, the estimation of actual pressures during implosion is very difficult and the average energy supplied to the pressure sensor is estimated instead. The energy flux supplied by pressure waves to the elementary area in an elementary period of time, associated with a single pressure pulse, is described by

$$I = \frac{p^2}{2Z} = \frac{p^2}{2\rho c_s}$$

where: $Z = \rho c_s$ – acoustic impedance, ρ - density, c_s – sound celerity , p – pressure pulse amplitude.

Thus, the density of an energy flux supplied to the material by imploding cavitation bubbles can be expected to be proportional to the following expression:

$$J = \frac{1}{T} \cdot \frac{1}{2\rho c_s} \sum_{k=1}^{M} n_k p_k^2$$

where T denotes duration of the pressure pulses sampling period, M – number of pressure intervals, n_k – number of pulses in a single interval, p_k – value of pressure amplitude in the k-th interval.

2. EXPERIMENTAL SET-UP

Experimental tests were performed in the Erdmann-Jesnitzer type cavitation tunnel in the laboratory of the Institute of Fluid–Flow Machinery, Polish Academy of Sciences, Gdańsk, Poland (Fig 1). The Erdmann-Jesnitzer test chamber enables to study erosion damage in different areas of cavitation cloud and at different cavitation intensities. The inlet and outlet pressure, the distance between the barricades and the position of the specimen can be adjusted. The cavities (cavitating vortices and bubbles) are generated due to the pressure decrease in the slot between two cylindrical barricades. Perspex windows on both sides of the chamber enable observation of the cavitation cloud fluctuations.

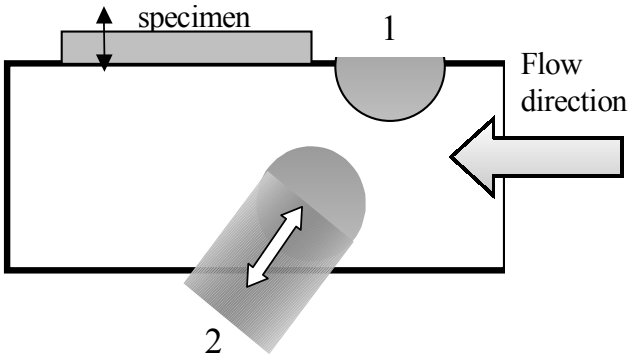

Fig.1 Schematic of the Erdmann-Jesnitzer type cavitation chamber in the IMP PAN lab: 1 – barricade, 2 – counter-barricade. The width of the slot between the barricades can be adjusted within the 0 ÷ 15 mm range.

Cavitation pulses were measured at different distance from the barricades, different inlet and reverse pressure and at different width of the slot. The inlet pressure was varied between 600 kPa and 1200 kPa, reverse pressure: between 110 kPa and 250 kPa, and the width of the slot: between 3 and 5 mm.

The specimens, each consisting of five adjacent sections, were subjected to cavitation erosion at three different flow parameters. First, erosion test was conducted at inlet pressure p_1= 600 kPa, reverse pressure p_2= 110 kPa and slot width equal δ = 3,8 mm, next at p_1 = 1000 kPa, p_2 = 110 kPa, δ =3,8mm, and finally at p_1= 1000 kPa, p_2= 120 kPa, δ = 5 mm. In the last case pits distribution was processed statistically after the first 315 s of exposure.

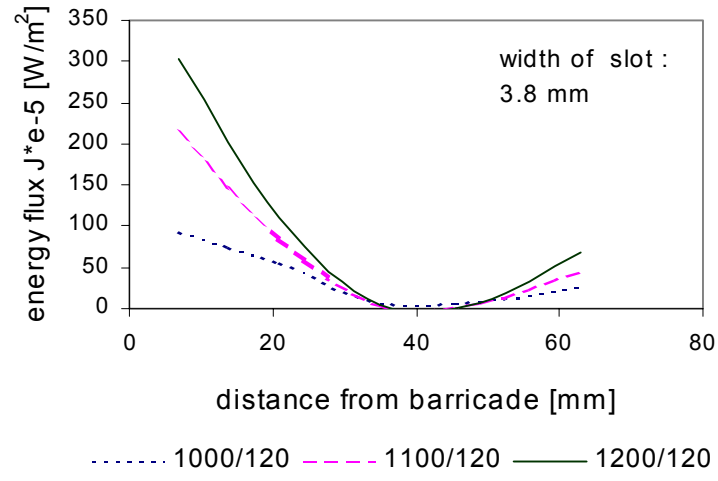

Fig.2 Relationship between the distance from the barricade and the energy flux density for different inlet pressures

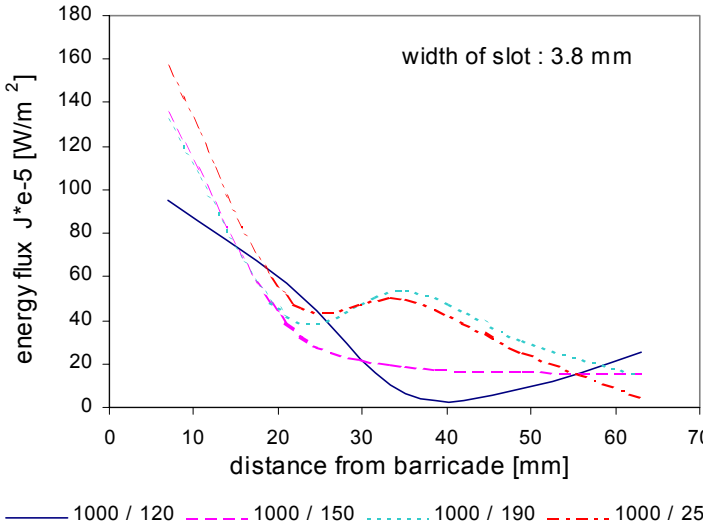

Fig.3 Relationship between the distance from the barricade and the energy flux density for different outlet pressures

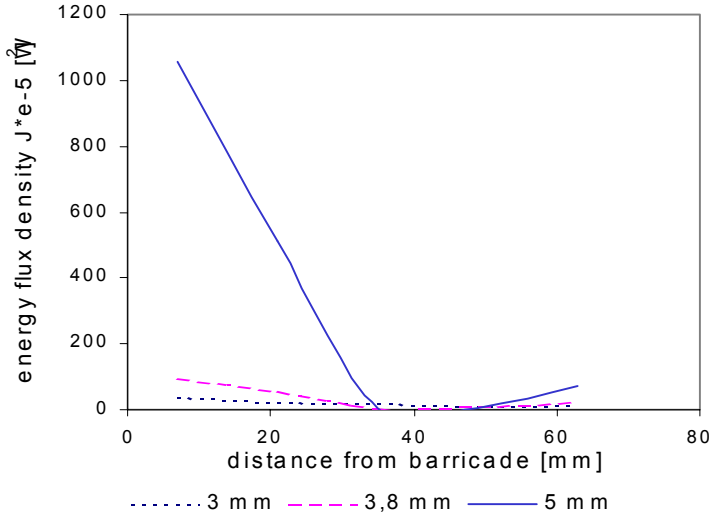

Fig.4 Relationship between the slot width and the energy flux density

3. MEASUREMENT OF PULSES

The obtained results are presented in form of relationship between the distance from the barricade and the energy flux density J (Fig.2). For fixed inlet pressure the highest *J* value was noted at the 7 mm distance from the barricade.

The highest fall of the energy flux density *J* occurs at the distance of 7 to 21 mm from the barricade. Further decrease is not so intense any more and the minimum value is reached at the distance of about 35 mm. At further distances, a slight increase of cavitation intensity is to be noticed. In case of inlet pressure being varied, cavitation intensity variation is not accompanied by any change in the cavitation cloud structure. Attainment of the minimum *J* value for all the pressure values p_1 at the same distance from the obstacle is clearly visible. On the other hand side, variation of the outlet pressure results in a shift of the cavitation intensity minimum towards the obstacle and a change of the cavitation cloud structure (Fig.3). This closely linked with development of the cavitation cloud vortex structure downstream of the obstacle.

Variation of the slot width exerts an essential effect on cavitation intensity. The change of slot width from 3.8 to 5 mm is accompanied by a tenfold increase of the energy flux density (Fig.4). The increase of the slot width at the same pressure values up- and downstream of the test chamber results in an increase of discharge and extension of the low-pressure area. This facilitates generation of a larger number of cavities, their growth and sudden expansion.

4. PA2 ALUMINIUM ALLOY MASS LOSSES AT VARIOUS VALUES OF THE ENERGY FLUX DENSITY PARAMETER

Specimens made out of the PA2 aluminium alloy have been subjected to cavitation impingement in an Erdmann-Jesnitzer test chamber at various flow conditions. At first, erosion tests were conducted at p_1 = 600 kPa, p_2 = 110 kPa pressures and 3.8 mm slot width. Then, pressures p_1 = 1000 kPa, p_2 = 120 kPa at 3.8 mm slot width and p_1 = 1000 kPa, p_2 = 120 kPa at 5 mm slot width were applied. Although cavitation cloud structure remained the same, different cavitation intensities have been attained (table 1).

a)

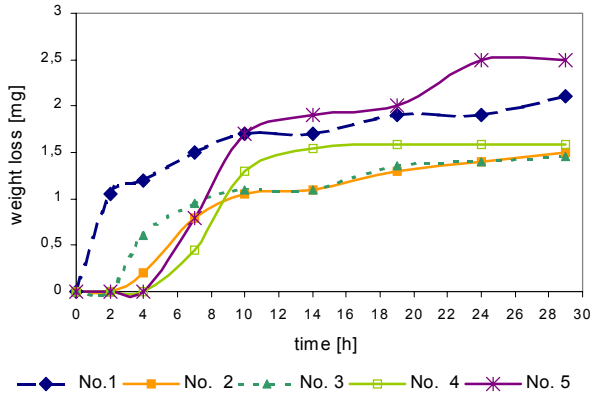

b)

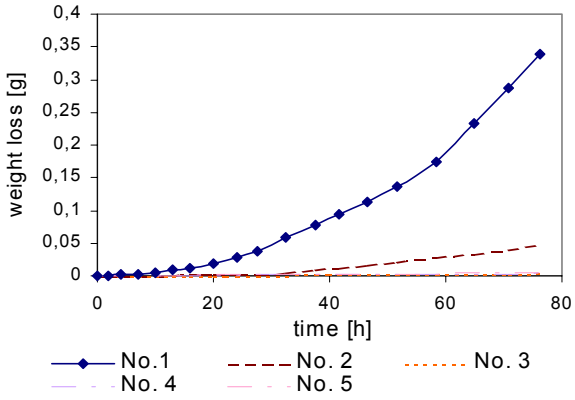

c)

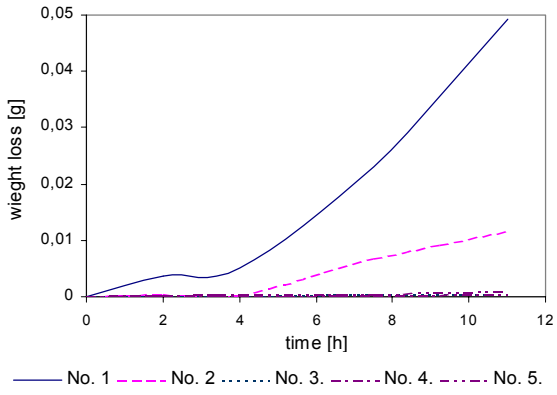

Fig.6 Erosion curves *a*) for p_1=600 kPa, p_2=110 kPa, width of slot 3.8 mm; *b*) for p_1=1000 kPa, p_2=110 kPa, width of slot 3.8 mm; *c*) for p_1=1000 kPa, p_2= 120 kPa, width of slot 5mm

Table 1 Energy flux density parameter along the specimen at different test conditions

Test conditions	*Energy flux density parameter J*E-5 [W/m²]*		
	7 mm	*21 mm*	*35 mm*
600/110 3,8 mm	13	0,1	1
1000/120 3,8 mm	33	9	0,5
1000/120 5 mm	1130	511	2,6

The change of energy flux density at 7 mm distance from the slot is most essential as that is the place where most of high-pressure pulses has been measured. These are the pulses of fundamental impact on the cavitation erosion progress.

PA2 aluminium alloy is a plastic material with high energy of location fault, high inclination for transversal slips and threadwise dislocations. These properties are linked to small value of tangential stress needed to produce plastic strain. Approximate value of this stress is

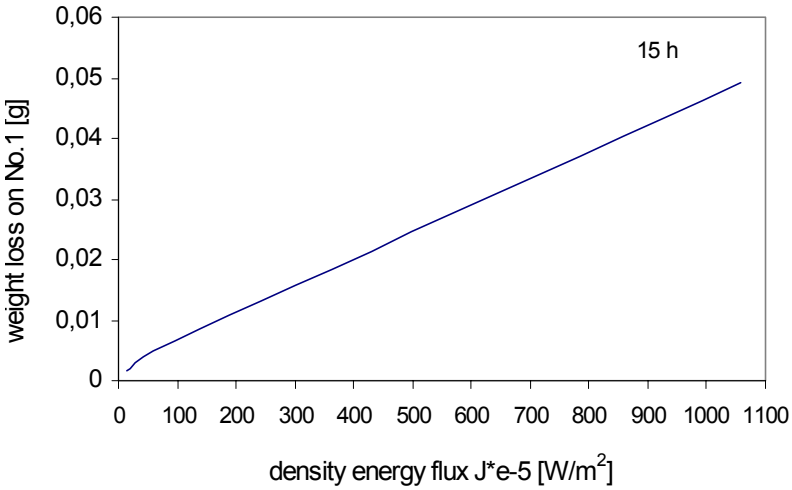

Fig.7 Relationship between the energy flux density parameter J and the weight loss of specimen No 1. after 15 h of exposure resulting (based on a series of 3 tests)

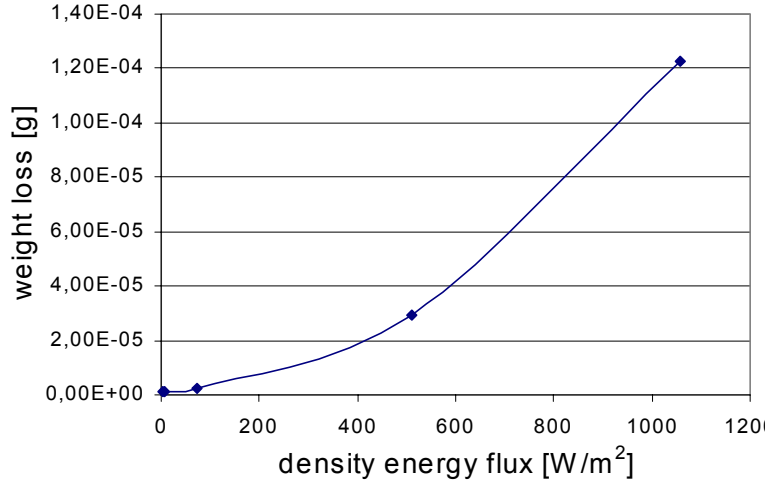

Fig.8 Relationship between the energy flux density parameter J and the mass loss determined for 5 specimens tested in one test series

comprised within the 1 ÷ 2 MPa range. Therefore, cavitation pulses of lower collapse pressure are not able to produce even a plastic deformation.

Cavitation erosion test results of the PA2 aluminium alloy are shown in Figs.6 and 7. Mass loss vs. time curves at p_1 = 600 kPa and p_2 =110 kPa pressures are comparable for all 5 specimens irrespective of the highest number of cavitation indentations stated at the first specimen section (which corresponds to the 0 ÷ 16 mm distance from the obstacle). One can suppose that the small differentiation of damage is due to lack high-pressure cavitation pulses.

The curve plotted in Fig.7 results from comparison of the mass losses at the first section with the density of the energy flux delivered to the specimen in all three test series after 30 hours of exposure. By comparing mass losses at all 5 specimen sections, tested in the same series, the curve shown in Fig.8 is obtained. One can suppose that in result of further tests, at more severe cavitation conditions, curve 7 will acquire an exponential pattern. Such a trend is consistent with the assumption that the high-pressure cavitation pulses - characterised by their frequency and amplitude - are of essential significance for the cavitation erosion progress.

5. MEASUREMENT OF CAVITATION PITS DEVELOPMENT

Development of cavitation pits at a PA2 alloy specimen with 80×45 mm size in the initial (incubation) cavitation erosion stage at p_1 =1000 kPa and p_2 = 120 kPa pressures has been analysed. The alloy was subjected to four consecutive exposures of 85 s duration each. After each exposure, observation at an optical microscope was carried out with magnification of 75:1. It follows from the observation that pits of 20 μm diameter generally prevailed. The state of the surface subjected to cavitation, and the shape and size of indentations in the mate-

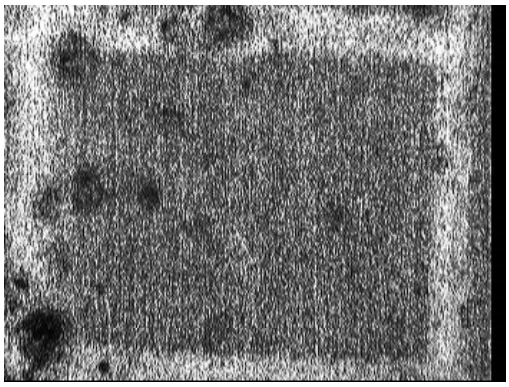

Fig.9. Image of the surface after 170 s of exposure (magnification 75 ×)

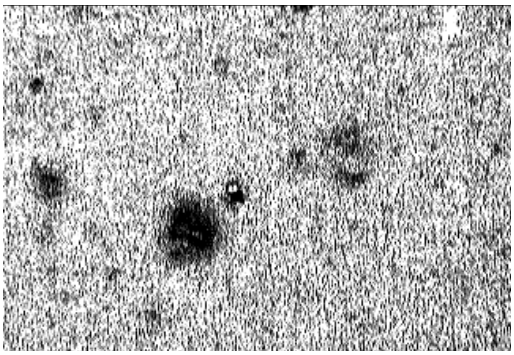

a) magnification 75 ×

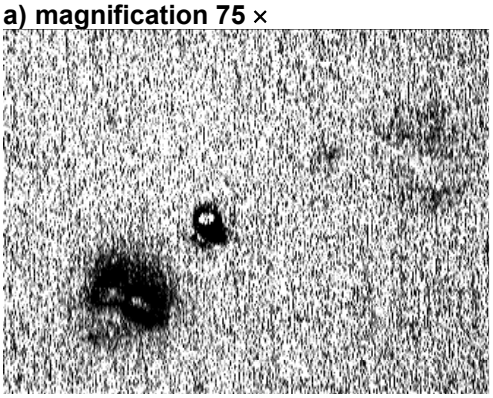

b) magnification 150 ×

Fig.10 The shape of an indentation consisting of two traces of cavitation bubbles collapse

rial due to collapsing cavities are depicted in Fig.9. It is worthwhile to notice that the indentation shown in Fig.10 seems to consist of a single pit when watched at 75× magnification (Fig.10a). However, when watching at 150× magnification one can easily discern two independent deformations, situated close to each other (Fig.10b). Pits formed by collapsing bubbles are featured by a characteristic ring shape with the undamaged central area. Such a shape is typical for collisions of small liquid jets with a solid.

These photographs show clearly the effect of the magnification applied. By applying too high magnification one can omit indentations of large diameter and small depth. On the other hand side, at low magnifications the smallest pits are invisible. Therefore in most cases one should expect that the counted number of pits is underestimated in respect to the realistic one.

By plotting the number of counted pits after 255 s and 315 s of exposure versus density of the energy flux delivered to the material, one receives the diagram shown in Fig.11. The average increment of the number of pits after every exposure was about 40 %, for higher cavitation intensities ($J = 1056*10^{-5}$ W/m^2) this increment is as large as 60 %. One should keep in mind that the counted number of pits is underestimated and the realistic increment of the number of pits is higher than that given in Fig.11. Adopting a logarithmic scale for the number of indentations yields a linear dependence, which proves good correlation between the number of pits and the energy flux density.

Fig.12 shows dependence between the largest diameters measured and the energy flux density after 170 and 315 seconds of exposure. The effect of the energy flux density and test duration on the size of largest pits is clearly visible. Also in this case one should keep in mind the underestimated values of the diameters measured. For $J = 1056*10^{-5}$ W/m^2 the increase of pit diameter was 60%, whereas the increase of only 4 5 % was obtained for $J = 521*10^{-5}$ W/m^2. Also in this case a linear dependence is obtained which proves good correlation of the largest pits formed in result of cavitation impingement.

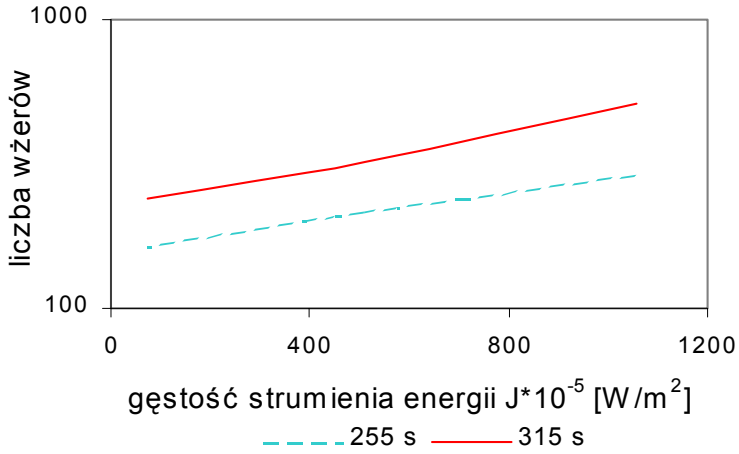

Fig.11 Dependence of the number of indentations on the energy flux density parameter

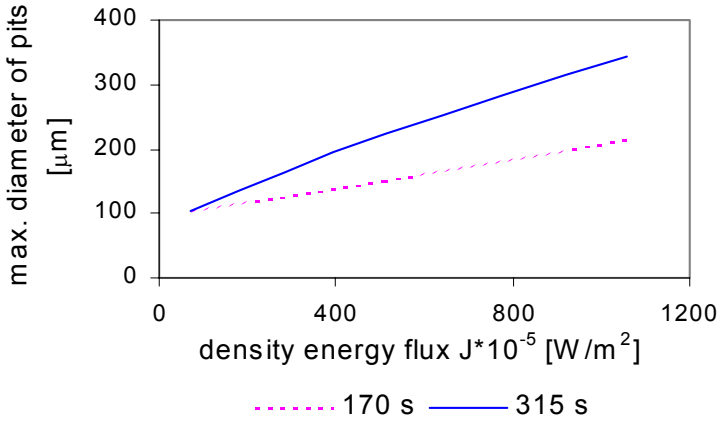

Fig.12. Dependence of the maximum cavitation pit diameter and the energy flux density parameter *J* after 170 s and 315 s of exposure

6. CONCLUSION

1. An increase of the p_1 pressure upstream the cavitation chamber at constant downstream pressure, p_2, results in an increase of the energy flux density J without noticeable change of the cavitation cloud structure. The minimum values of the *J* parameter were measured at the distance of 40 mm from the obstacle. Scarce differentiation of these values has been stated.
2. An increase of p_2 pressure downstream of the chamber at constant p_1 pressure is accompanied by a change of the cloud structure. A shift of the minimum *J* value towards the obstacle and an increase of the energy flux close to the obstacle have been stated.
3. An increase of the energy flux density is accompanied by an increase of mass losses after 15 hours of exposure. The mass loss vs. energy flux density curve tends to show an exponential pattern.
4. An increase of the energy flux density is accompanied by an increase of the number of pits formed in result of cavitation impingement.
5. An increase of the energy flux density is accompanied by an increase of the maximum pit diameter. The dependence tends to show a linear character.
6. The relationships derived show significant dependence between the number of high-pressure cavitation pulses and the material damage due to cavitation.